Hail Day Frequency Trends and Associated Atmospheric Circulation Patterns over China during 1960–2012

MINGXIN LI AND QINGHONG ZHANG

Department of Atmospheric and Oceanic Sciences, School of Physics, Peking University, Beijing, China, and Department of Meteorology, and Center for Advanced Data Assimilation and Predictability Techniques, The Pennsylvania State University, University Park, Pennsylvania

FUQING ZHANG

Department of Meteorology, and Center for Advanced Data Assimilation and Predictability Techniques, The Pennsylvania State University, University Park, Pennsylvania

(Manuscript received 20 July 2015, in final form 6 July 2016)

ABSTRACT

Based on a comprehensive collection of hail observations and the NCEP–NCAR reanalyses from 1960 to 2012, the long-term trends of hail day frequency in mainland China and the associated changes in atmospheric circulation patterns were analyzed. There was no detectable trend in hail frequency from 1960 to the early 1980s, but a significant decreasing trend was apparent in later periods throughout most of China and in particular over the Tibetan Plateau from the early 1980s and over northern and northwestern China from the early 1990s. Hail frequency in southern China did not decrease as significantly as in other regions over the last couple of decades. An objective classification method, the obliquely rotated T-mode principal component technique, was used to investigate atmospheric circulation patterns. It was found that 51.85% of the hail days occurred during two major circulation types, both of which were associated with cold frontal systems in northern China. More specifically, the synoptic trough in East Asia, signified by the meridional circulation at 850 hPa, became considerably weaker after 1990. This change in the synoptic pattern is consistent with a weakening trend in the East Asian summer monsoon, the primary dynamic forcing of moisture transport that contributes to the generation of severe convection in northern China. The long-term variability of hail day frequency over the Tibetan Plateau was more strongly correlated with the change in mean freezing-level height (FLH) than the strength of the East Asian monsoon.

1. Introduction

Hail is a type of extreme precipitation in the form of balls or irregular lumps of ice produced by convective clouds (Changnon 1978). When hail occurs, it can cause losses to crops, vehicles, and houses. The high velocity of large volumes of ice reaching the ground can also be extremely dangerous to people and animals (Cao 2008); for example, agricultural losses caused by hailstorms and other severe convection in China reached 31.55 billion CNY in 2012, which exceeded the damage caused by tropical cyclones (China Meteorological Administration 2012). An understanding of long-term trends in hail frequency may provide useful information for governments and society to reduce economic losses.

As a kind of extreme weather, hail has been studied in several different regions worldwide, in terms of both climatology and its long-term trend. Tuovinen et al. (2009) showed that hail damage and hail days in Finland have significantly increased over the last three decades, although this increase was attributed mostly to the increase of severe-hail reports along with improved communications technology, as well as the public and media's greater interest in severe weather. Using hail damage data from a building insurance company, Kunz et al. (2009) found that the number of severe-hail events

Denotes Open Access content.

Corresponding author address: Prof. Qinghong Zhang, Department of Atmospheric and Oceanic Sciences, School of Physics, Peking University, Beijing 100871, China.
E-mail: qzhang@pku.edu.cn

DOI: 10.1175/JCLI-D-15-0500.1

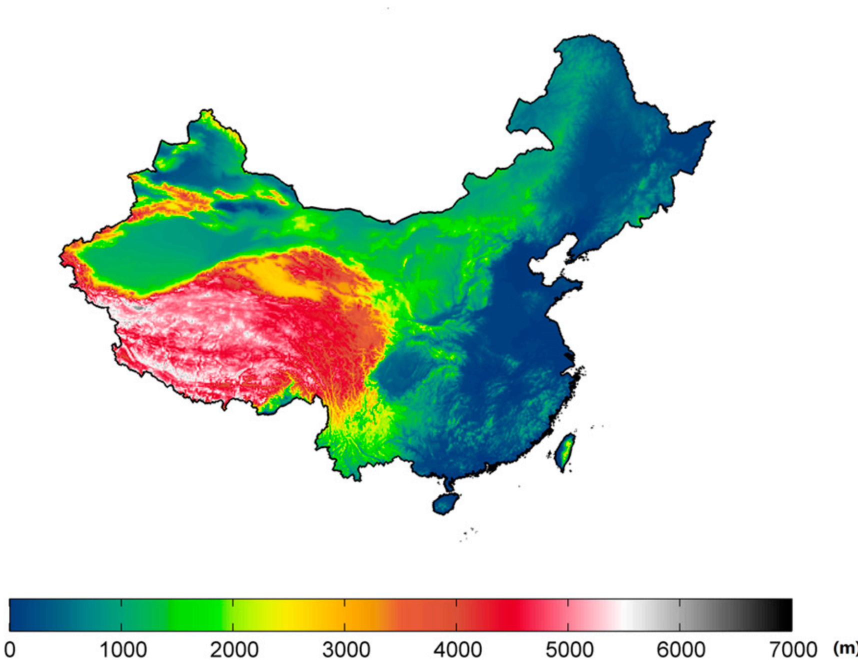

FIG. 1. Topography of China. Shading is terrain height.

and severe-hail days has been increasing since the late 1990s in Germany, which may also be affected by the inhomogeneous distribution of population. In addition, a robust increase in the frequency of severe-hail events has also been reported over Ontario, Canada, since 1982 (Cao 2008). Using the Severe Weather Database provided by the Storm Prediction Center (SPC), Allen and Tippett (2015) showed a strong upward trend of observed hail days for hail diameter larger than 0.75 inches over the contiguous United States. However, this does not correspond to a significant trend in the number of days with hail reports since the 1990s. Moreover, there is little evidence in directly relating these changes to changes in the large-scale atmospheric environment (Allen et al. 2015). However, quite different results have been reported in some other countries. In Sydney, Australia, hailstorms were less frequent from 1989 to 2002 than during the preceding 36 years, whereas regions outside Sydney experienced an increase in hailstorms and hail days, which is likely attributable to increased reporting (Schuster et al. 2005). China has also experienced a significant downward trend in annual hail days since the early 1980s based on a large number of stations with daily human observations (Xie et al. 2008). A recent study reported that most stations in North Korea have experienced a sharp decline in hail activity from 1981 to 2010 (Kim and Ni 2014). Whether the number of hailstorms has changed and the reasons why hail frequency has changed remain an area of active research.

China occupies the eastern part of the vast Eurasian continent, with the world's highest plateau (the Tibetan Plateau) and a variety of topography and landscapes (the topography of China is shown in Fig. 1), all of which contribute to the regional diversity of hailstorm climatology (Zhang et al. 2008). There have been several studies of hail climatology in China. Hail can occur almost everywhere in the country, except for a few areas in the southern and eastern plains (Liu and Tang 1966; Zhang et al. 2008). The long-term trend of annual hail days in China shows a decrease since the 1980s (Xie et al. 2008). How and why the hail day frequency changes under global and regional climate change in China is still unknown.

However, there is an apparent difficulty in correlating the local-scale hail occurrence with global climate change. Surface hail observations are not accurate because direct monitoring systems are unable to record all hail activity. Because of the coarse temporal and spatial resolutions (Cecil and Blankenship 2012), along with the inaccuracy in using the overshooting tops as a hail proxy, satellite data also do not always describe hail accurately. Using the maximum expected size of hail derived from the multiradar multisensor (MRMS) algorithm, Cintineo et al. (2012) provide an improved estimate of hail climatology given the high spatial resolution, but such radar-based estimates have limited skill for large hail sizes and have poor temporal coverage. Numerical weather forecasts lack the ability to explicitly and reliably simulate deep convection owing to both the temporal and spatial resolution as well as the unknown physical processes (Noppel et al. 2010). Nevertheless, the environmental conditions that favor hail-producing severe convection, such as convective available potential energy (CAPE), vertical wind shear (VWS), and freezing-level height (FLH), may be associated with a synoptic flow shift under conditions of global climate change. For example, Allen et al. (2015) developed an empirical model relating the monthly occurrence of hail to large-scale environmental conditions, which matches the annual cycle of hail occurrence and spatial distribution for the United States. Xie et al. (2008) found that the decreasing hail trend in China was associated with a rising trend in the mean FLH in China during 1960–2005, although this may reflect only the situation in the mountainous area. Moreover, as the formation of small-scale convection usually needs the support of large-scale circulation, connecting hailstorm occurrence to more specific large-scale circulation patterns can help us to understand changes in hail frequency and its response to climate change.

Several studies have been conducted in European countries to classify hailstorms based on the circulation type. Kapsch et al. (2012) found a relationship between days with damaging hail and specific weather types, and the number of hail-related weather types increased slightly from 1979 to 2000 in Germany when using an objective method. Kunz et al. (2009) also found an increase in the southwesterly weather type, which was strongly related to the number of hail days in Germany when a subjective classification method was applied. Different methods were used to investigate hailstorms in Lleida (Catalonia), and it was found that objective classification has an advantage over manual classification for hailstorms (Aran et al. 2011). Current studies in China have limitations in time and space and use subjective methods that may involve multiple criteria (Wang et al. 2010; Ji et al. 2007; Yu et al. 2004a).

To overcome the disadvantages of the subjective methods mentioned above, an objective classification method was used in this study. Objective classifications play an important role in atmospheric circulation classification and can be implemented through airmass classification or circulation-based classification (both types are defined, and cases are assigned, by a numerical procedure; Huth et al. 2008). Local meteorological variables are closely interrelated, which sometimes can be extensively influenced by large-scale circulations (Zhang et al. 2012). Because the aim of this study was to explore the influences of atmospheric circulation on hail frequency, the circulation-based classification system was used to classify circulation types.

This study focused on the long-term change in hail frequency and its relationship with large-scale circulation patterns in mainland China. The datasets and methodology are described in section 2. Section 3 gives a description of hail climatology and the long-term changes in hail frequency in China. Section 4 shows the results of the classification of circulation patterns and their relation to hail frequency changes. A discussion is provided in section 5, which is followed by a summary in section 6.

2. Dataset and methodology

The hail data used here were obtained from the National Meteorological Information Center (NMIC), which has a complete historical hail dataset of 753 stations over mainland China from 1951 to 2012. If a hailstorm is recorded at one station on a particular day, we defined it as a hail day for this station. Because of the continuity of meteorological data and the relatively large data record, we excluded stations that were relocated. If one station had more than 10 missing data points in a single month, that month was considered to be an invalid month for that station. Stations with at least one invalid month were not used in the analysis. As a result, 541 stations with complete records from 1960 to 2012 were selected to ensure a relatively large and continuous data record (Fig. 2). The National Centers for Environmental Prediction–National Center for Atmospheric Research (NCEP–NCAR) reanalyses of daily mean sea level pressure (SLP) and geopotential height were used for objective analyses of flow pattern changes. The daily mean relative humidity, air temperature, geopotential height, wind field, surface temperature, surface pressure, and surface relative humidity from the NCEP–NCAR reanalyses were used to calculate convective inhibition (CIN), CAPE, VWS (calculated as the magnitude of wind vector difference between 500 and 850 hPa), and FLH.

There have been several studies examining the climatology of hail in China. After Liu and Tang (1966) showed the spatial distribution and seasonal cycle of China's hailstorms from 1950 to 1960, Zhang et al. (2008) extended the hail climatology data to 2005. Both studies found that hail frequency in northern China was higher than in southern China and that the hail season has a diverse geographical distribution in China. The current study further extends the hail data to 2012. Figure 2 gives a general description of the seasonal and spatial variation in hail occurrence found in this study. Annual mean hail days decreased from north to south and from west to east, which was strongly related to topography (Fig. 1). The highest

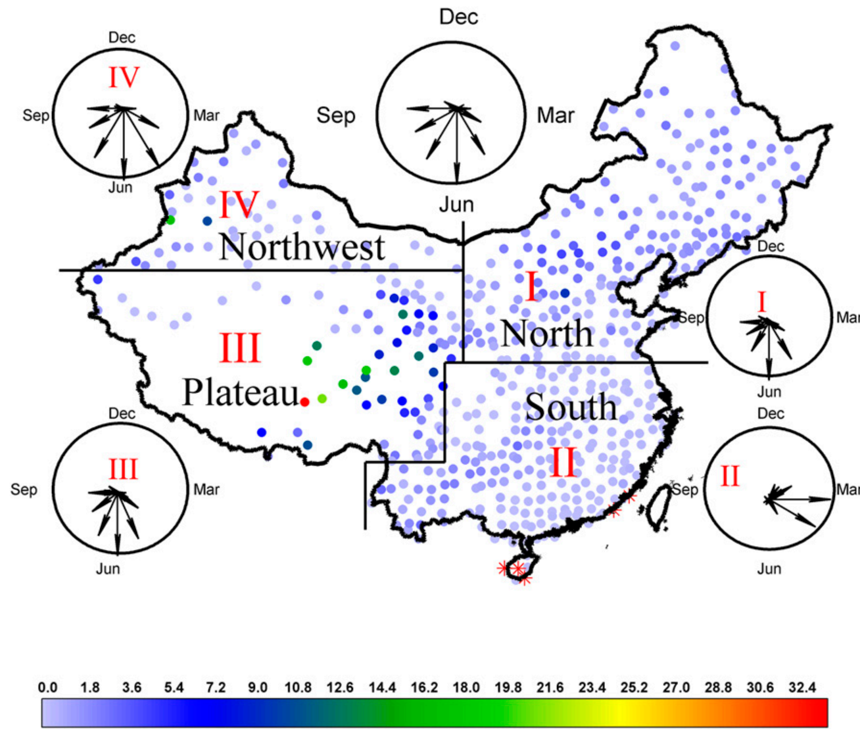

FIG. 2. The distribution and annual mean hail days of 541 stations from 1960 to 2012 (color dots represent annual mean hail day frequency). Four subareas are marked with I, II, III, and IV; circles indicate the monthly variation of hail days for each subarea (indicated by the red roman numerals) or the whole nation (length of the arrow represents ratio of monthly hail frequency to annual hail frequency, and direction of arrow shows the month). Red asterisks mark the stations where no hail has ever been observed.

number of annual hail days occurred in the Tibetan Plateau. Hail occurred mainly in the cold season in the south and in the warm season for the rest of China, which was consistent with the results of Zhang et al. (2008). The synoptic systems that influence the western and eastern parts of China are different (Wang et al. 2010; Ji et al. 2007; Yu et al. 2004a). Taking both the spatial and seasonal distribution into account, we defined four regions: the north, the south, the plateau, and the northwest regions, marked as I, II, III, and IV, respectively, in Fig. 2. The study period in the north, plateau, and northwest regions was from April to October, which was broadly categorized as the warm season in this study. For the south region, hail in the cold season was studied instead. The cold season months for the south are loosely defined as from January to May and from November to December. When focusing on either the warm seasons or the cold seasons (but not the entire year), more stations meeting the data requirements could be selected for the four regions, which resulted in a total of 199, 227, 77, and 47 stations for the north, south, plateau, and northwest regions, respectively.

The obliquely rotated T-mode principal component analysis (PCT; where the columns of the input data represent time observations and rows correspond to grid points) proposed by Huth (1993) was used in this paper. This method is capable of capturing the underlying physical structure (e.g., it can reproduce the predefined circulation types when applied to an existing phenomenon as a capability test), and the results were found to have more stability in time and space than other objective classification methods. It can also effectively avoid the ‘‘snowballing’’ effect (i.e., forming one huge cluster to which an increasing number of other groups are attached in later stages of the clustering, accompanied by small clusters and unclassified days) compared to other methods (Huth 1996a,b). The method we used here was developed within the framework of COST Action 733 (http://cost733.met.no/; Huth et al. 2008; Philipp et al. 2010, 2014). A brief summary of PCT is given below. Readers interested in the details of the method can refer to Huth (1996a,b, 2000).

There are two possibilities for arranging the input data field, which correspond to T-mode PCA and

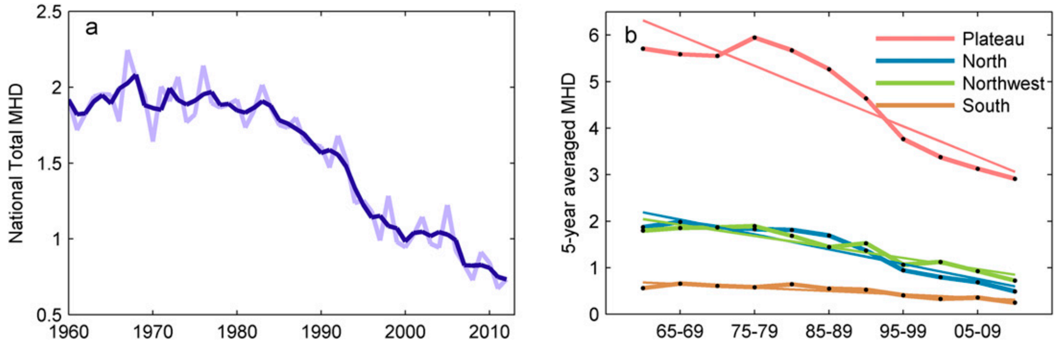

FIG. 3. (a) MHD of China during 1960–2012 (light blue) and its moving average (dark blue). (b) The 5-yr average MHD and trend line of four regions (red represents the plateau, blue represents the north, green represents the northwest, and yellow represents the south).

S-mode PCA, respectively. In T-mode PCA, the gridpoint values are in rows and cases (time realizations) are in columns. In S-mode, grid points are organized in columns and cases are in rows. With the requirement that the principal components (PCs) should usually be rotated if PCA is to be used for classification purposes (Richman 1986), significant difference between the two modes becomes apparent. Each rotated loading is required to contain many near-zero elements, while the remaining loadings frequently have high absolute value (close to one). In S mode, the loadings can be interpreted as maps of a particular PC and the scores describe the temporal variation of the PC. In contrast, the loadings in T mode describe the temporal evolution of the PCs. Each PC on a particular day either ''occurs'' (loading close to one) or does not (loading close to zero). Thus, it is easy to classify each day pattern to the type for which it has the highest loading. The ''clusters'' sought by the rotated PCs in the phase space from T-mode PCA correspond to the circulation types. It is therefore obvious that the T-mode PCA may provide a classification of circulation patterns rather than the S mode (Huth 1996a,b).

3. Long-term trend and variation of hail days in China

Xie et al. (2008) first showed the long-term trend of hail occurrence in China and found a significant downward trend from 1980 to 2005. After extending the comprehensive hail data to 2012, we found a continuous significant decrease in the annual station mean hail days (MHD) from the early 1980s for the whole of China (Fig. 3). However, the long-term variations of annual MHD were different among the four separate regions. We followed the method of Changnon and Changnon (2000), which used the temporal distributions of the ten 5-yr values for the four regions (the 11th point was the average of the last 3 years because the data covered a period of 53 years). Figure 3b shows that all four regions had experienced a significant decrease over several decades. The trend was $-0.3251\,(5\,\mathrm{yr})^{-1}$ for the plateau, $-0.1592\,(5\,\mathrm{yr})^{-1}$ for the north, $-0.1194\,(5\,\mathrm{yr})^{-1}$ for the northwest, and $-0.0371\,(5\,\mathrm{yr})^{-1}$ for the south. Compared to the other three regions, the decrease in the MHD in the south accounted for the smallest share of the total decrease in MHD. The annual MHD in northern China remained constant from the 1960s to the 1980s but then started to decrease in the early 1990s. The annual MHD in northwestern China also decreased, but with considerable interannual variability. Unlike in the north and northwest, the annual MHD in the plateau increased slightly in the early 1970s, peaked in the late 1970s, and began to decline in the 1980s. The annual MHD in the plateau declined 10 years earlier than in northern China. When considering Figs. 3a and 3b together, the decline in the annual MHD over China after the 1980s was primarily due to a decrease in the north, northwest, and plateau regions.

Figure 4 shows the trend of annual hail days for each station calculated from 1960 to 2012. It was found that 37.8% of stations had a significant decreasing trend and 49.1% stations displayed a nonsignificant decreasing trend. In addition, 12% of stations displayed an increasing but nonstatistically significant trend. Compared with the results of a study of hail in China from 1960 to 2005 (Xie et al. 2008), more stations displayed a decreasing trend in annual hail days and there was almost no station that displayed a significant upward trend in the longer-term dataset.

With regard to the spatial distribution, most stations that had a decreasing trend in annual hail days were located in northern China. The maximum in the downward trend of annual hail days was located in the

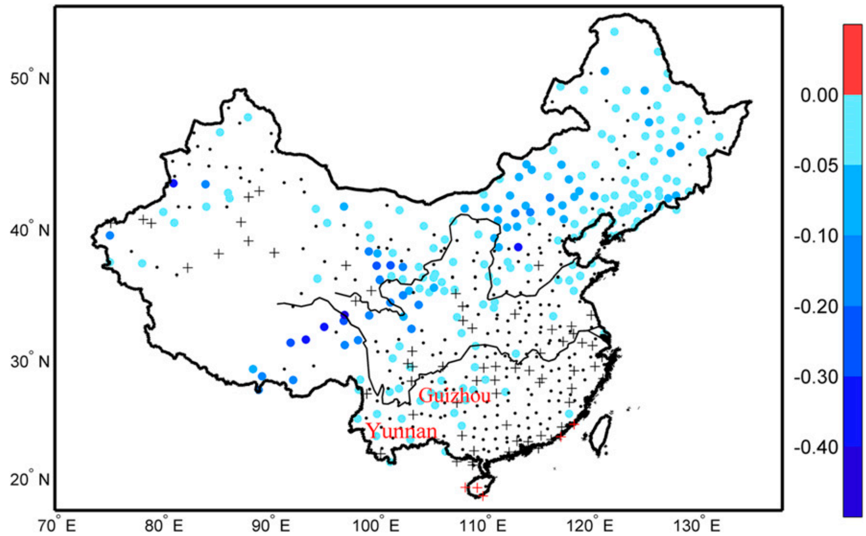

FIG. 4. Annual hail day trend (day yr^{-1}) of 541 stations during 1960–2012 [colored dots represent stations with significant trend at 0.05 level, and colors represent the trend value. Black dots and black plus signs represent stations with downward or upward trend (but not significant); red plus signs represent stations with no hail days observed].

plateau area. The majority of stations in southern China displayed no trend, except for several in Yunnan and Guizhou provinces (marked in Fig. 4). Stations located in the plateau and mountainous areas tended to have a downward trend in annual hail days. In general, the trend in annual hail days reduced from northern to southern China and from western to eastern China, which was strongly related to the unique terrain configurations across the country. These regional differences in long-term hail day trends suggest potential variations in the local atmospheric circulations and conditions favorable to hail development.

4. Atmospheric circulation patterns with hail in China

In this section, we provide an objective classification of large-scale circulation patterns during the study period. We analyzed the change in frequency of hail days for each circulation type and determined the circulation types that favor hailstorms. We also investigated differences in the circulation features between hail days and nonhail days. Finally, we attempt to explain the overall decreasing trend in hail day frequency in China from 1960 to 2012.

Over the study period, there were a total of 11 342 days included for classification during the warm season. Given that northern China and the plateau were responsible for the largest decline in hail day frequency and that the northwestern region had a very limited number of stations, our analysis focused on northern China and the (Tibetan) plateau region.

a. Northern China

The spatial patterns of the geopotential height at 500 hPa (20°–60°N, 70°–135°E) were classified into five types using PCT. The corresponding geopotential heights at 850 hPa and sea level pressure for each of the five circulation types for northern China are shown in Fig. 5. At the 500-hPa geopotential height field, the main difference among the five different circulation types was the position and strength of the East Asia trough. With the trough located to the east of northern China, circulation types 1-N (N represents north) and 4-N resulted in a wide area of high sea level pressure in northern China. Circulation type 2-N was characterized by a strong trough, with the trough axis at ~105°E and the corresponding SLP field displaying a strong low centered in northeastern China. Circulation type 3-N was characterized by a shallow trough located in northeastern China with widespread low pressure at sea level. Both circulation types 2-N and 3-N displayed meridional circulations at 850 hPa, while the trough corresponded well with the spatial pattern at 500 hPa. Circulation type 5-N was characterized by straight East Asia westerlies and a much weaker trough at 850 hPa, along with a weaker pressure gradient at sea level.

Because the circulation frequency differed, we calculated the hail occurrence ratio as the total number of hail days at a specific station under one circulation type divided by the total number of days of the corresponding spatial

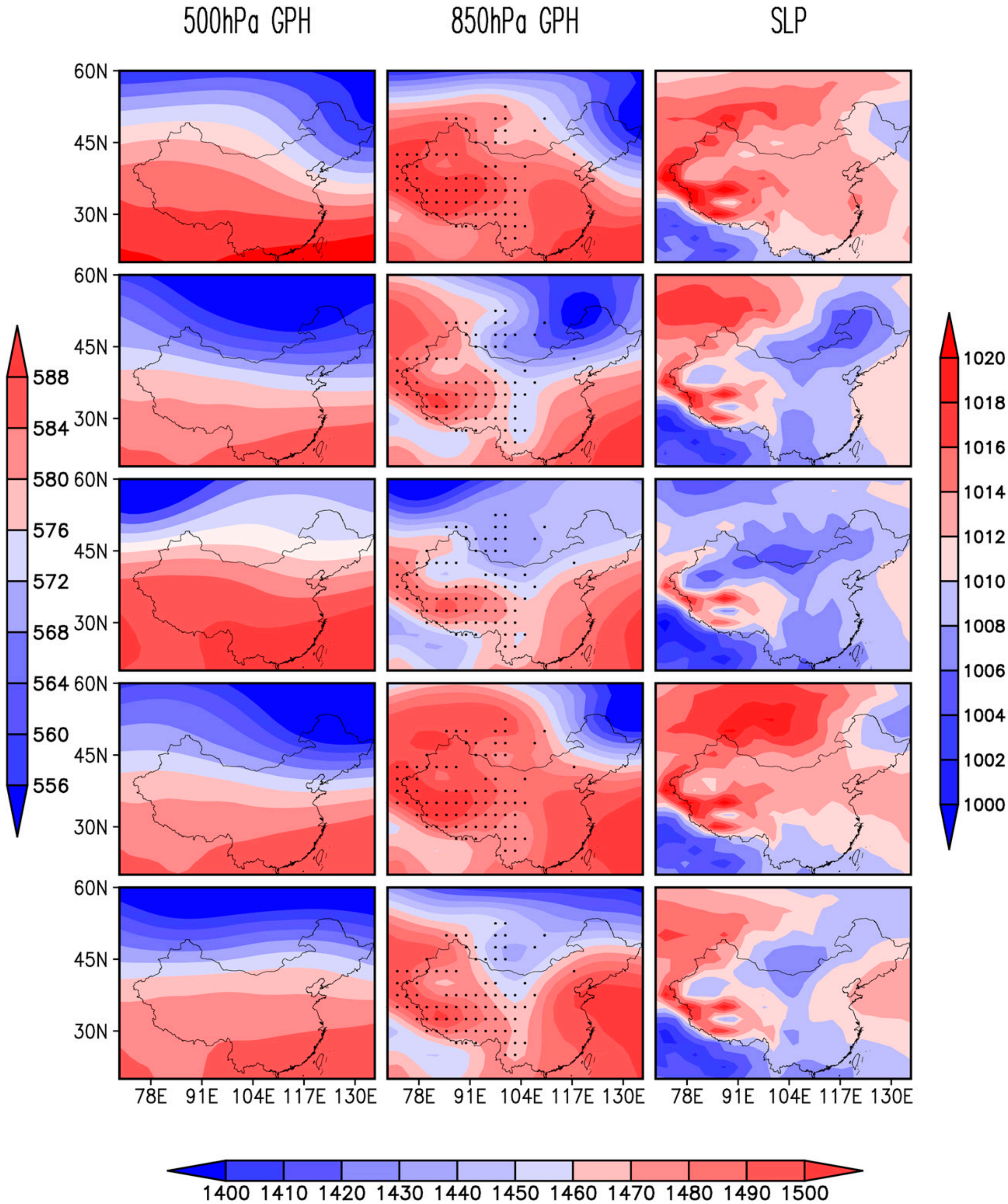

FIG. 5. (left) The 500 hPa geopotential height (10 m), (center) 850 hPa geopotential height (m), and (right) SLP (hPa) of five circulation types in northern China in warm season during 1960–2012. Black dots in (center) represent the area where 850-hPa geopotential height is lower than topography altitude. (from top to bottom) Type 1-N, type 2-N, type 3-N, type 4-N, and type 5-N.

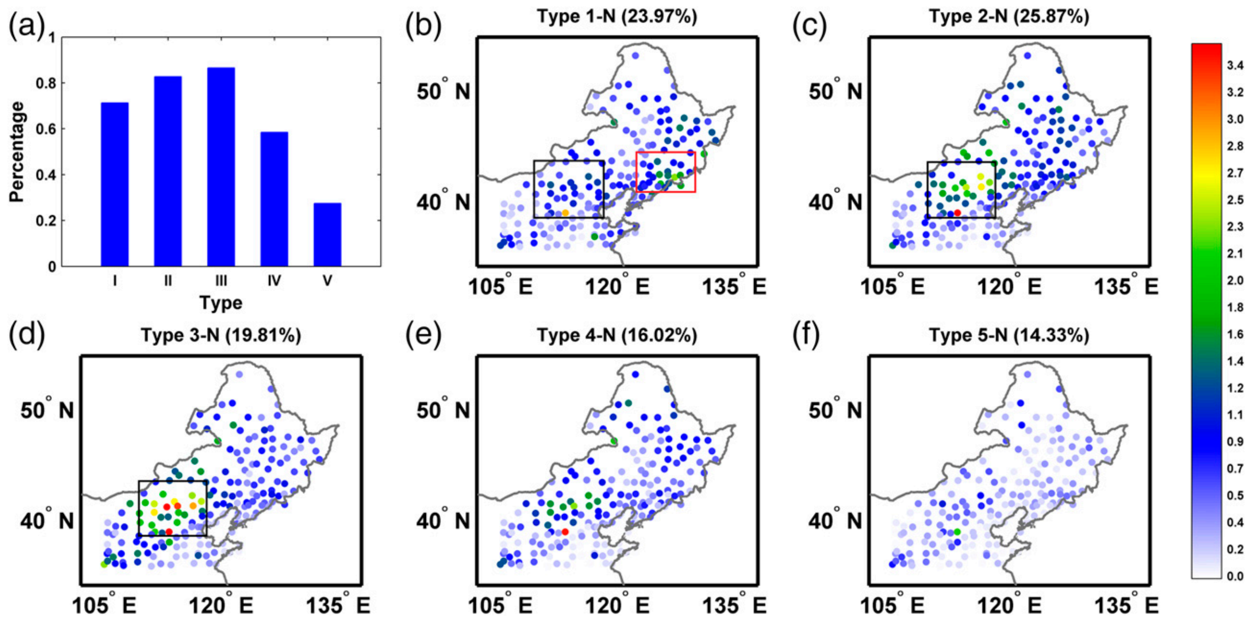

FIG. 6. (a) Station mean hail occurrence ratio for the five circulation types (%) and (b)–(f) spatial distribution of hail occurrence ratio for the five circulation types in the warm season during 1960–2012. In (b)–(f), the color represents the value of ratio; black box marks Inner Mongolia and red box marks the northeastern part.

pattern (Fig. 6). The blue bars in Fig. 6a are the station mean hail day occurrence ratios (sum of the hail day occurrence ratio under one circulation type divided by the station number in northern China) under the five circulation types. Hailstorms happened most frequently in circulation type 3-N, followed by types 2-N, 1-N, 4-N, and 5-N. The numbers above Figs. 6b–f represent the frequency of each circulation type over the entire warm season. It can be seen that of all five circulation types, type 2-N occurred most frequently. Hail occurred in the whole area, with a relatively high frequency under circulation types 2-N and 3-N. Under all circulation types, the eastern part of Inner Mongolia (marked with the black box in Figs. 6b–d) always has a high hail occurrence. Circulation type 1-N was more unusual, with significantly more hailstorms occurring in the northeast compared to Inner Mongolia. Under circulation type 1-N, when the East Asia trough was located farther south at a relatively low latitude together with a low pressure system moving just out of northeastern China, more hailstorms occurred in the northeast (marked with a red box in Fig. 6b) rather than Inner Mongolia. Under circulation type 3-N, when the low pressure center was located at 45°N, 104°E (i.e., a more eastward position), hailstorms mainly occurred in Inner Mongolia. The displacement of the area where hail was concentrated indicated that the storms producing the hail occurred on the trailing front, which was physically sensitive to the location of the front. The first three circulation types appear to represent the evolution of a large-scale synoptic wave passage. As the low pressure center moved eastward, the area of maximum hail occurrence area shifted from Inner Mongolia to the northeast. Overall, hail days in northern China were more likely to occur during the passage of frontal and postfrontal systems, as typified by the flow configurations of circulation types 2-N and 3-N.

From the time series of the frequency of circulation types in northern China, a strong interannual variation of the circulation types was apparent. However, there was no obvious long-term trend in the frequency of each circulation type that correlated with the downward trend in hailstorm frequency in the early 1990s. Nevertheless, the hail occurrence ratios were considerably lower than the averages from the 1990s (as the blue vertical line indicates in Fig. 7). Focusing on the two dominant flow patterns, we examine the sea level pressure composition fields of circulation types 2-N and 3-N before and after the 1990s (shown in Fig. 8). It is evident that the low-level pattern after the 1990s became weaker than in the period before 1990, indicating weaker convergence and potential for moisture advection. This also reflects a decrease in the system's dynamics, under which the environmental conditions do not favor the occurrence of hail, which could be one reason for the downward trend in hail day frequency in northern China. Favorable environments for deep convection can be broken down into three components: VWS, thermodynamic propensity, and a process for convective initiation (Tippett et al. 2015). Based on these three

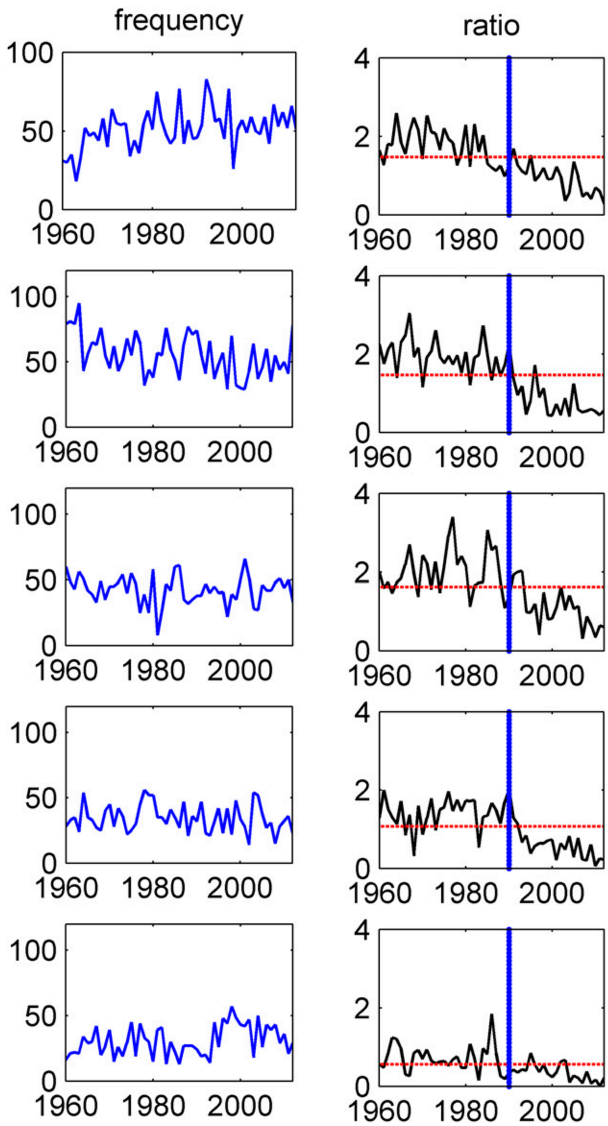

FIG. 7. Time series of (left) circulation type frequency and (right) hail occurrence ratio under each type in the warm season from 1960 to 2012; red line is time average, and blue vertical line shows the year of 1990.

aspects and the formation and melting processes of hail, we considered CIN, CAPE, VWS, and FLH to be the main parameters influencing hail. CIN is the energy needed against stratification to lift an air parcel from its original position to its level of free convection. When the air parcel overcomes CIN and reaches its level of free convection, CAPE is released and the parcel can realize its latent instability. To analyze this, we calculated the annual mean occurrence of CIN for the two periods 1960–89 and 1990–2012 under circulation types 2-N and 3-N. The results shown in Fig. 9 indicate that after the 1990s, CIN increased. The increased CIN made it more difficult for hailstorms to initiate. This is in agreement with the results of Zhao et al. (2006), who demonstrated that the number of unstable days significantly decreased from 1986 to 2003 by calculating CAPE minus CIN as the index of unstable days. CIN is closely related to surface and lower-troposphere temperature. Myoung and Nielsen-Gammon (2010) showed that warming at 700 hPa and surface dryness combined to produce large CIN leading to precipitation deficits on a monthly time scale in summer in Texas and that CIN modified the number of rain days more than the intensity. Both the surface and lower-troposphere temperature have displayed an increasing trend over the globe (Klotzbach et al. 2009; Brown et al. 2000). A potential explanation for this increased CIN could be the warming lower-tropospheric temperatures. In addition to CIN, the annual mean occurrence of CAPE, VWS, and FLH (Fig. 9) were also calculated. There was a decrease in the average CAPE for circulation type 2-N and no clear change for circulation type 3-N. Considering that large hail typically occurs in extreme instability environments, the annual mean occurrence of CAPE with extremely large values after 1980 does not change much under type 2-N even though the average CAPE decreases. VWS changed little for both circulation types. The mean FLH for circulation type 2-N decreased after 1990 and increased slightly for circulation type 3-N. The decreased hail day frequency was more related to CIN than the other indices. The increased CIN tended to stabilize the atmosphere after the 1990s, and it became more difficult for air parcels to be lifted to initiate hailstorms.

Considering that the hail day frequency under all five flow types has decreased, which can be seen clearly in Fig. 7, we examined the changes in flow pattern for all types together. Figure 10 shows the composites at 500 (Fig. 10a) and 850 hPa (Fig. 10b) for the entire study period. The black contour represents the geopotential height when hail occurred (to obtain the obvious characteristics of circulation when a hailstorm occurred, we considered days when more than five stations experienced a hailstorm to be a hail circulation day and combined these days to obtain a circulation composite), while the shaded color shows the difference (hail circulation day minus nonhail circulation day). It can be clearly seen that the 500-hPa geopotential height composite for the hail circulation days had a deeper trough located in northeastern China. This was more obvious in the 850-hPa geopotential height, where there was an even larger difference. As shown in Fig. 11a, the difference in the focus area was dominated by an anticyclonic high center after the 1990s, which indicates a weaker dynamic forcing for hail generation. Together with Fig. 11b at the upper level,

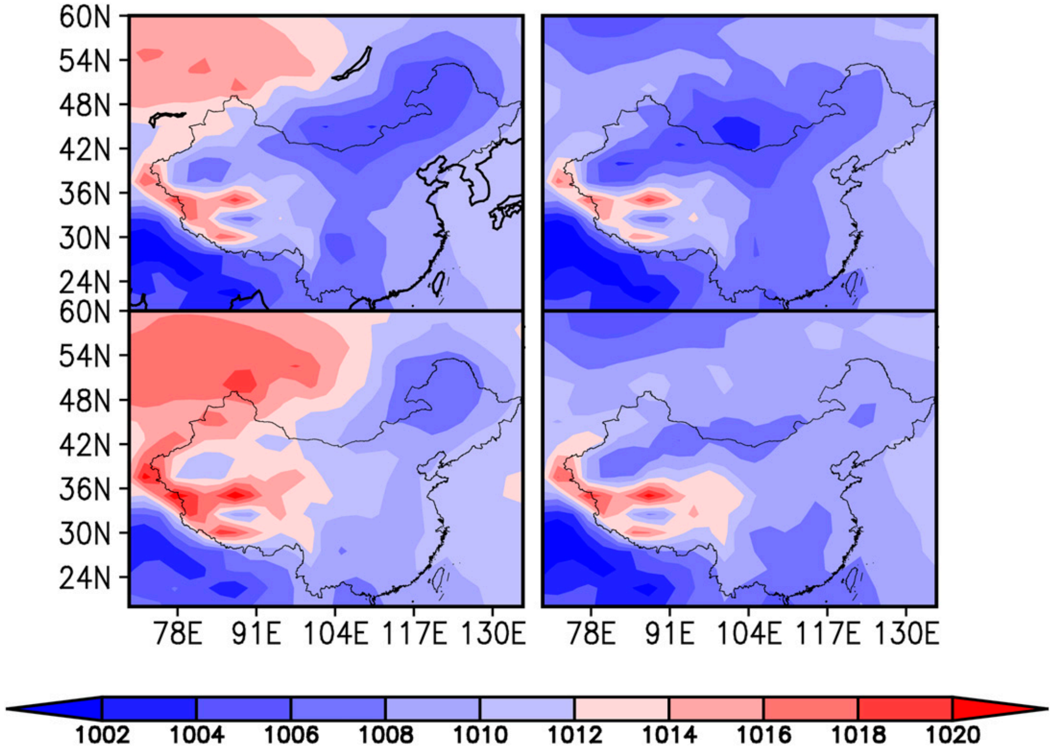

FIG. 8. Composite SLP (hPa) under (left) type 2-N and (right) type 3-N during (top) 1960–89 and (bottom) 1990–2012.

we can clearly see that the trough located in central China considerably weakened after the 1990s. The vorticity of the two periods (not shown) also showed a decrease in the dynamic forcing. Meanwhile, the meridional component of wind (Fig. 12) weakened after 1990, bringing less moisture to northern China, which further contributed to the decrease in hail day frequency. This change in pattern has also been considered to be the primary reason for the decreased annual extreme precipitation in northern China (Wang and Zhou 2005). Similarly, Ding et al. (2008) and Yu et al. (2004b) also found a significant weakening of the East Asian summer monsoon together with northward moisture movement and convergence weakened by the summer monsoon. This has led to a deficient moisture supply for precipitation and a tendency toward increased droughts in northern China, which appears to also influence hail occurrence.

b. The Tibetan Plateau region

The Tibetan Plateau is the world's highest plateau, with an average elevation of more than 4000 m above sea level. To avoid the incomplete atmospheric data–related signals around the plateau, the 500-hPa geopotential height field was used for the classification of PCT type and the 700-hPa geopotential height field was used for the composite analysis over the plateau region shown in Fig. 13. The five circulation types differ from one another in location, intensity, and shape of the upper-level trough. The synoptic situations were similar between 500 and 700 hPa for all circulation types. Circulation type 1-P was the most frequent circulation type, accounting for 45.66% of the total on all days. The percentage contributions of the other types were 22.5%, 12.62%, 10.18%, and 9.02%. From the spatial distribution of the hail occurrence ratio (Fig. 14), it could be seen that hailstorms occurred for every circulation type and with much higher ratios than over northern China. There was a slightly higher hail day frequency in circulation types 4-P and 5-P because there was a trough located upstream of the plateau area at 500 hPa. This was more obviously reflected in the 700-hPa levels, where the short-wave trough was located to the northeast of the plateau, which would bring cold air and lead to instability when cooperating with the warm air near the surface. Circulation types 4-P and 5-P accounted for only 19.2% of all circulation types, which means that in the plateau area the main circulation types (1-P, 2-P, and 3-P) all had a hail day frequency ratio of around 2%. The hail day frequency ratio under circulation types 4-P and 5-P were both about 2.5%. The hail day frequency in the plateau was much higher than in the other regions and was increased if the synoptic trough in the upper level

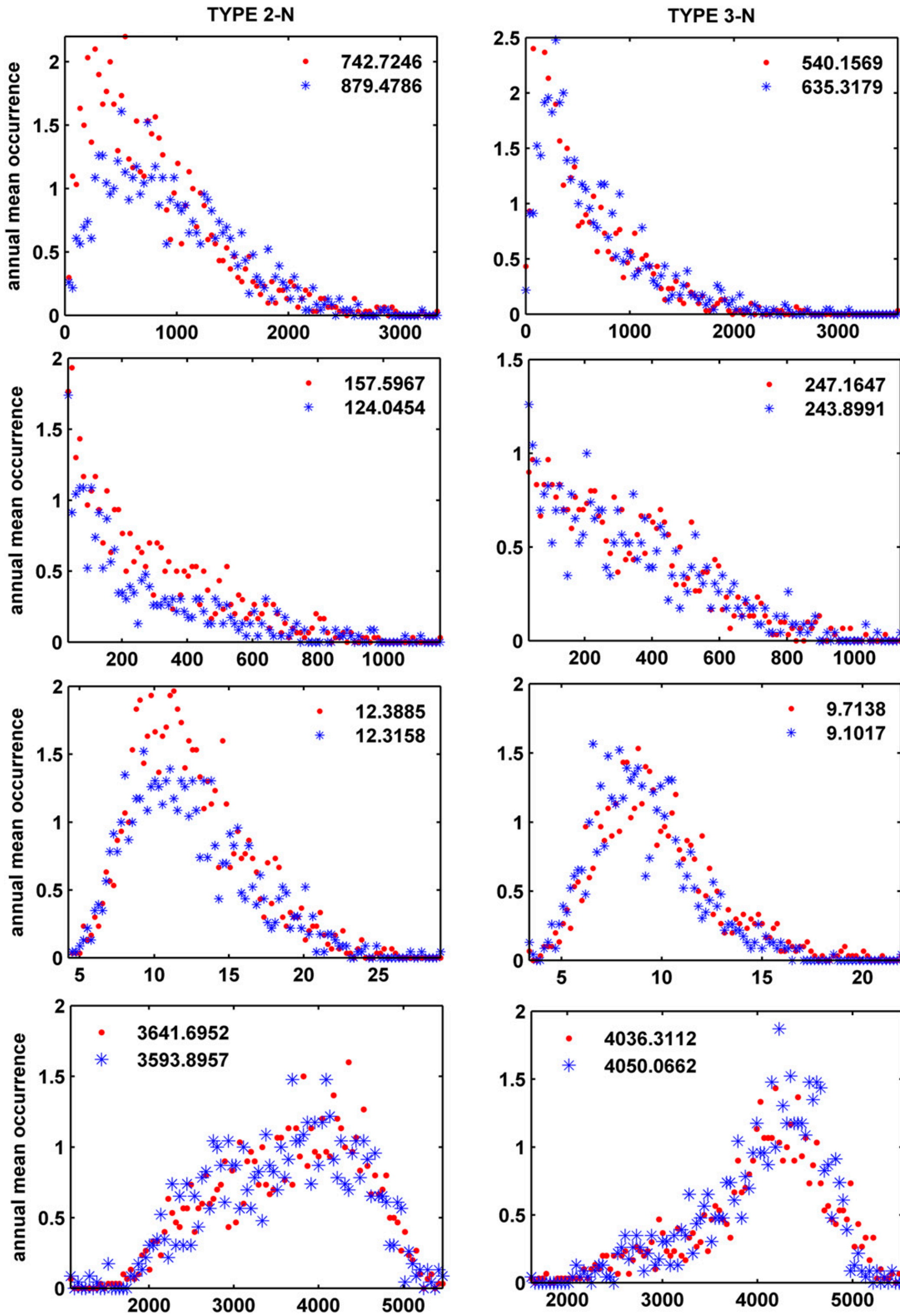

FIG. 9. Annual mean occurrence of (from top to bottom) CIN (J kg^{-1}), CAPE (J kg^{-1}), VWS (m s^{-1}), and FLH (m) in the warm season during 1960–89 (red dots) and 1990–2012 (blue asterisks) under (left) type 2-N and (right) type 3-N (legend shows the mean value of the two periods).

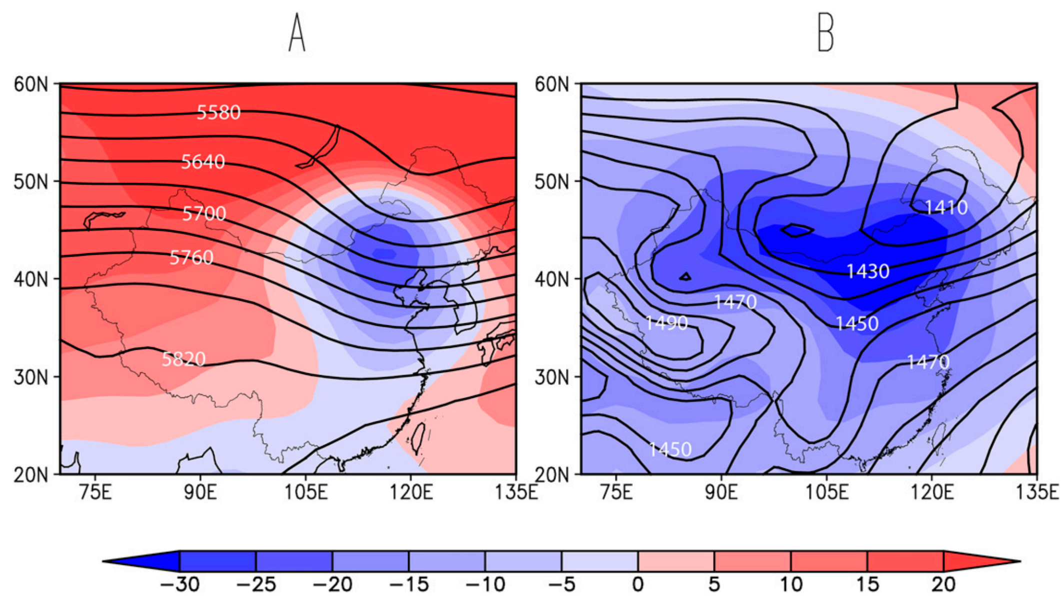

FIG. 10. Composite of (a) 500- and (b) 850-hPa geopotential height (m) of hail circulation days (black contour); shaded color shows the difference on 500- and 850-hPa geopotential height (m) of hail circulation days and nonhail circulation days for northern China in warm season from 1960 to 2012.

brought cold air to cooperate with warm air near the surface, although this circulation type accounted for less than 20% of all circulation types. From this perspective, circulation type had an effect on plateau hail formation, but it was not as significant as in northern China because of the relatively low occurrence of such circulation types and the high hail day frequency under the other main circulation types. To some degree, circulation patterns had an influence on hailstorms in the Tibetan Plateau region, but the effects were not as important as in northern China.

5. Discussion

As mentioned above, many factors may contribute to the formation of hail, among which topography and atmospheric circulation influenced by topography play important roles (Vinet 2001). Doswell et al. (1996)

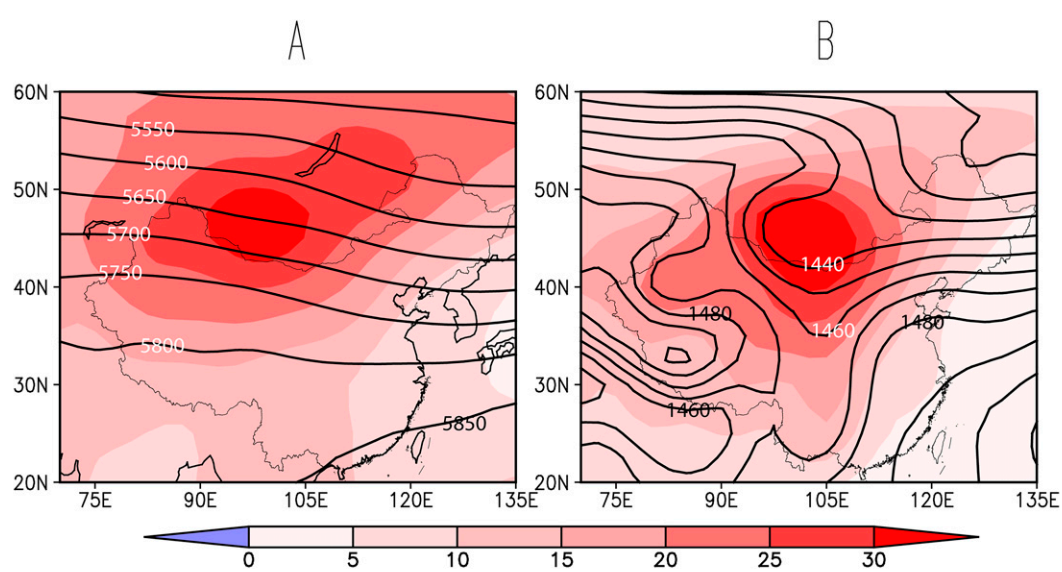

FIG. 11. Composite of warm season (a) 500- and (b) 850-hPa geopotential height (m) from 1960 to 1989 (black) and the difference (m) between periods 1960–89 and 1990–2012 (color shading).

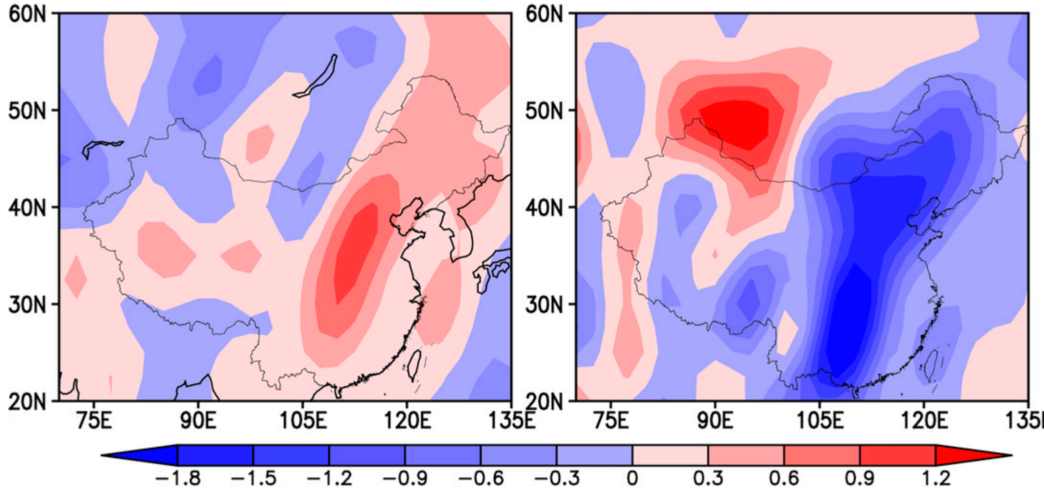

FIG. 12. Meridional wind difference (m s^{-1}) of warm season 850-hPa geopotential height (left) between hail circulation day and nonhail circulation days and (right) between periods 1960–89 and 1990–2012.

summarized the factors leading to heavy precipitation according to three aspects: large-scale processes, mesoscale processes, and storm-scale processes. Modest but persistent synoptic-scale vertical ascent ahead of shortwave troughs creates the moistening and destabilization needed for deep moist convection. Mesoscale processes provide the lifting needed for the initiation of convection and the mesoscale terrain is an important lifting mechanism. In addition, the evolution of a convective event can be modified significantly by the convection itself through the outflow created by convective downdrafts.

As shown in Figs. 5 and 6, large-scale frontal and postfrontal systems are the main factors associated with the occurrence of hail away from the Tibetan Plateau. When the cold front systems became weaker after the 1990s, the occurrence of hailstorms in northern China clearly decreased. The trough in the upper levels was considerably weakened, leading to weak synoptic-scale vertical motion, which had a large effect on the moisture and destabilization needed for deep convection. The decreased meridional wind also resulted in less moisture and thus less instability. The increased convective inhibition made it harder for convection to be generated because it needed a stronger trigger to overcome CIN after the 1990s. In addition to these factors, VWS was also a crucial factor that affected hail formation. Brooks (2013) showed that the intensity of tornadoes and hail in the United States tends to be almost entirely a function of the shear and only weakly depends on the thermodynamics. The role of VWS is especially crucial for large hail (Johnson and Sugden 2014; Allen et al. 2015); however, in northern China, hailstorms mainly produce small hailstones (mean hail diameter in most stations in the north ranges between 5 and 10 mm; figure not shown here). The VWS in China is much weaker than in the United States and seems to have played a less important role in the decreased trend in hail day frequency because the VWS for the stations with no obvious decrease in the hail day frequency trend also weakened (Xie et al. 2008). This might indicate differences in the importance of VWS between China and the United States.

The frequency of hail day in the plateau region was high under all circulation patterns. The circulation patterns had less influence on hailstorms in the Tibetan Plateau region than in northern China. This can be explained by the more isolated convective cells over the plateau than nearby regions and the dominance of convective clouds caused by solar insolation (Fu et al. 2006), which concurs with the observation that unstable air masses lead to the development of isolated hail and thunderstorms noted by Changnon and Changnon (2000). Under such circumstances where local solar insolation plays such an important role, CIN and CAPE are analyzed for periods 1960–79 and 1980–2012 over the plateau (Fig. 15). Although the amount of average CIN increase after 1980 is not as much as that in northern China, it plays a role in hail day frequency decrease in the plateau. CAPE increased little and thus can be neglected as a significant cause of the downward trend in hail days. The FLH is a crucial factor for hail formation, and is heavily affected by the solar insolation effects caused by the topography in the plateau area. Hail normally forms above the freezing level through complicated cloud microphysical processes. On the one hand, if the FLH is low enough for liquid drops to remain above it, there is a greater chance that hail will form. Alternatively, when falling from a cold cloud, ice

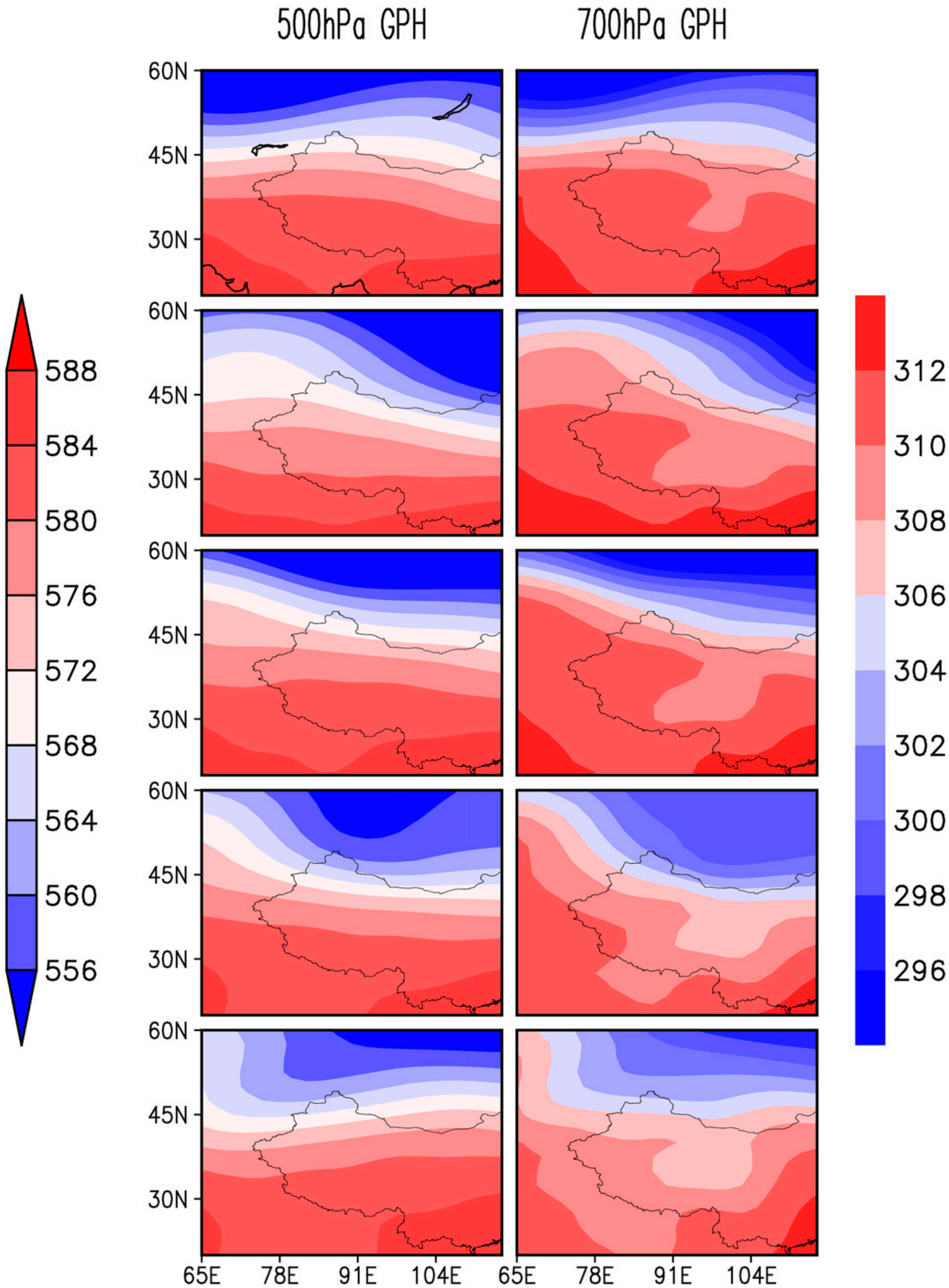

FIG. 13. Circulation type of the plateau: (left) 500-hPa geopotential height (10 m) and (right) corresponding 700-hPa composition (10 m) in the warm season of 1960–2012; (from top to bottom) type 1-P, type 2-P, type 3-P, type 4-P, and type 5-P.

will melt less before it reaches the ground; thus, hail occurs. The effects of FLH become more significant in mountain areas and for small hail stones. Hail size in the plateau region is mainly small (<5 mm; figure not shown here), which is very relevant to the melting process. The FLH decreased slightly between 1970 and 1980 (Fig. 16), which corresponded to a brief period of increased hailstorms in the Tibetan Plateau region. There was a

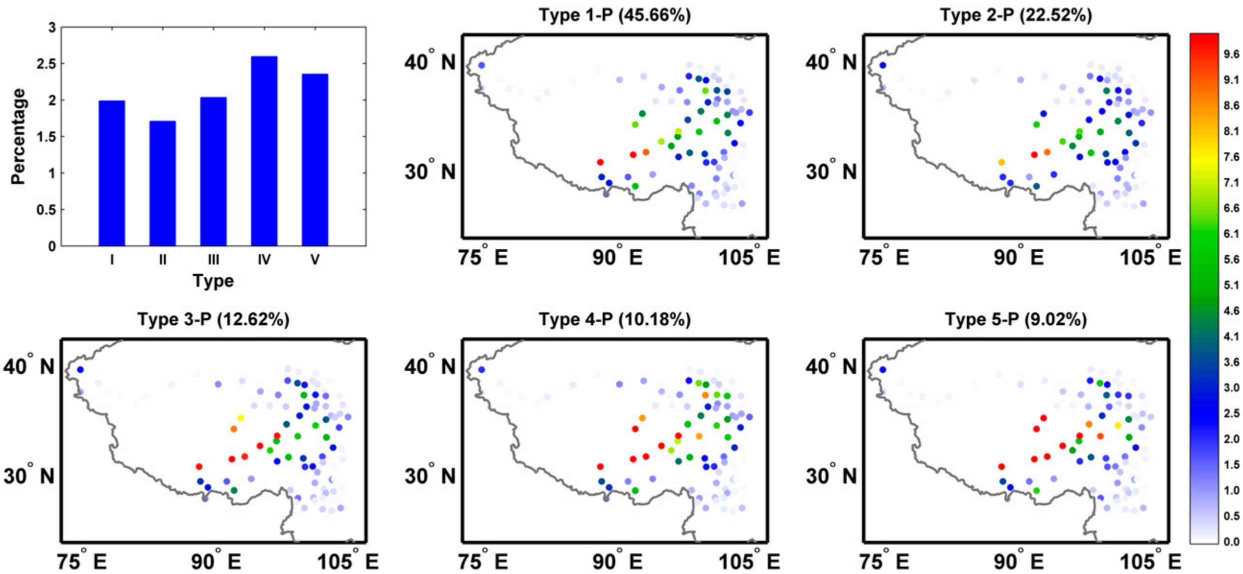

FIG. 14. As in Fig. 6, but for the plateau area.

negative correlation of −0.3531 between the warm season mean FLH and MHD for the plateau region, which was significant at the 99% confidence level. This further supports the hypothesis that the FLH is a crucial factor in the formation of small hail over mountains and that hail in the plateau is largely related to changes in the FLH.

By serving as cloud condensation nuclei (CCN) and affecting the size distribution of cloud droplets (Rosinski and Kerrigan 1969), aerosols may also play a significant role that cannot be neglected. Some studies have found that an increase in the aerosol concentration leads to the formation of smaller droplets (Khain et al. 2005). In contrast, Loftus and Cotton (2014) found that an increase in the CCN leads to greater predicted hail sizes and more large-diameter hail stones. Thus, aerosol effects on hail day frequency remain an active area of research. The long-term trend of hail day frequency in China may be affected by aerosols, and this is not fully understood. Nevertheless, the effects of increasing CCN on the dynamics and precipitation of deep convection can also depend on environmental conditions, as well as the type of convection (Khain et al. 2004, 2005). The circulation pattern classification performed here may therefore help us to differentiate between favorable synoptic situations, even if we cannot fully understand the impact of other factors, such as aerosols.

The occurrence of hail in China is closely related to terrain configurations. Almost all of the areas where hail is concentrated are mountainous (Zhang et al. 2008), because a high topography provides a favorable background for air lifting and can produce differential heating (Thielen and Gadian 1997). Hail formation in the Tibetan Plateau is even more complicated. Thunderstorms in the

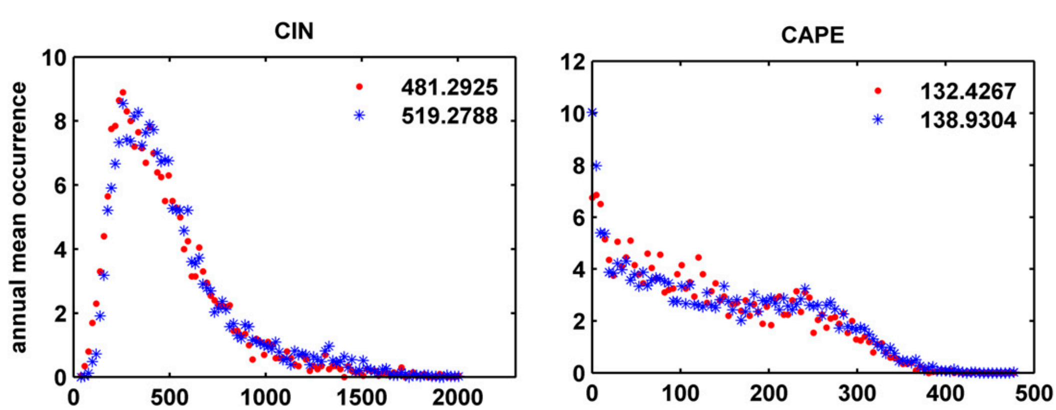

FIG. 15. Annual mean occurrence of (left) CIN and (right) CAPE in the warm season during 1960–79 (red dots) and 1980–2012 (blue asterisks) for plateau area (legend shows the mean value of the two periods).

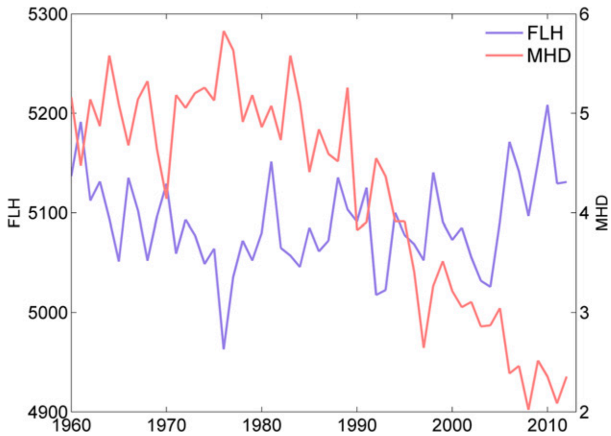

FIG. 16. Variation of mean FLH (m; dark blue) and MHD (pink) of the plateau in the warm season from 1960 to 2012.

plateau are strongly related to the terrain and the heating effect it produces. More isolated cloud cells are found over the plateau than in nearby regions (Fu et al. 2006). The initiation and development of severe mesoscale convective systems over the plateau is mainly driven by its thermotopographic effect (Jiang and Xiang 1996). We believe that the thermodynamic and dynamic processes from topographic effects are much more significant than synoptic flow, although it is beyond the scope of this study to completely separate the influences of the different factors. The sensitivity of hail in the plateau to the FLH is evidence of such terrain altitude effects. Both the slight increase (1970s) and the earlier decrease (1980s) of hail day frequency in the plateau show the causes of changes in the frequency of hail day may be different from other regions. It is also reasonable to expect that the plateau's response to climate change may occur sooner than in its neighboring areas or in the same latitudinal zones because this region is likely to be very sensitive to global climate change (Liu and Chen 2000). The occurrence of hailstorms in the plateau region is determined by unique local factors, and the insensitivity to circulation patterns is an interesting phenomenon. Because we focused on the effects of synoptic systems in this study, the details of the plateau hailstorms will be the focus of our future work.

6. Conclusions

A comprehensive collection of hail observations provided by the NMIC and NCEP–NCAR reanalyses from 1960 to 2012 were used here to analyze the long-term trends of hail frequency in mainland China and the associated changes in atmospheric circulation patterns. There was no detectable trend in hail day frequency from 1960 to the early 1980s, but a significant decreasing trend for the annual MHD was observed in later periods across all of China. When considering hail day frequency separately, a downward trend in the annual MHD in the Tibetan Plateau started from the early 1980s, while in northern and northwestern China it started from the early 1990s. Annual MHD in southern China did not decrease as significantly as in three other regions over the last couple of decades. In terms of the spatial distribution, 37.8% of stations displayed a significant decreasing trend in annual hail days. These stations were mainly located in the north and plateau regions, which were strongly related to the unique terrain configurations in China. Stations in the south had no significant trend, and no station in China displayed an increasing trend.

An objective classification method was used to investigate the atmospheric circulation patterns. Five circulation patterns were obtained with PCT. The results showed that 51.85% of the hail days in northern China occurred during two major circulation types (2-N and 3-N), both of which were associated with low-level low pressure systems. More specifically, they both had deep troughs at 500 hPa and a meridional circulation at 850 hPa, with a low pressure system at sea level pressure but with different strengths and locations. The synoptic trough in East Asia, signified by the meridional circulation at 850 hPa, weakened considerably after the 1990s along with a weakening in the meridional wind over eastern China. This change in the synoptic pattern was consistent with a weakening trend in the East Asian summer monsoon, which was considered to be the primary dynamic forcing with moisture transport that contributed to hail generation in northern China. In addition, the increase of CIN in northern China tended to stabilize the atmosphere and made it more difficult for the air parcel to be lifted. Short-wave troughs upstream of the plateau area increase the chance that hailstorms happen. But this synoptic effect is not as significant as over northern China. Both the increased CIN and FLH contribute to hail day frequency decline after 1980 in the plateau area. The long-term variation in hail frequency over the Tibetan Plateau correlated well with the variation of mean FLH rather than the strength of the East Asian monsoon. Further model sensitivity studies should be considered to explain the changes of hail day frequency.

Acknowledgments. This study is supported by the Chinese National Science Foundation under Grants 41330421 and 41461164006. The authors also acknowledge the editor and anonymous reviewers, whose valuable comments and suggestions significantly improved this article.

REFERENCES

Allen, J. T., and M. K. Tippett, 2015: The characteristics of United States hail reports: 1955–2014. *Electron. J. Severe Storms Meteor.*, **10** (3), 1–31.

——, ——, and A. H. Sobel, 2015: An empirical model relating U.S. monthly hail occurrence to large-scale meteorological environment. *J. Adv. Model. Earth Syst.*, **7**, 226–243, doi:10.1002/2014MS000397.

Aran, M., J. Pena, and M. Torà, 2011: Atmospheric circulation patterns associated with hail events in Lleida (Catalonia). *Atmos. Res.*, **100**, 428–438, doi:10.1016/j.atmosres.2010.10.029.

Brooks, H. E., 2013: Severe thunderstorms and climate change. *Atmos. Res.*, **123**, 129–138, doi:10.1016/j.atmosres.2012.04.002.

Brown, S. J., D. E. Parker, C. K. Folland, and I. Macadam, 2000: Decadal variability in the lower-tropospheric lapse rate. *Geophys. Res. Lett.*, **27**, 997–1000, doi:10.1029/1999GL011174.

Cao, Z., 2008: Severe hail frequency over Ontario, Canada: Recent trend and variability. *Geophys. Res. Lett.*, **35**, L14803, doi:10.1029/2008GL034888.

Cecil, D. J., and C. B. Blankenship, 2012: Toward a global climatology of severe hailstorms as estimated by satellite passive microwave imagers. *J. Climate*, **25**, 687–703, doi:10.1175/JCLI-D-11-00130.1.

Changnon, S. A., 1978: The climatology of hail in North America. *Hail: A Review of Hail Science and Hail Suppression*, *Meteor. Monogr.*, No. 38, Amer. Meteor. Soc., 107–128.

——, and D. Changnon, 2000: Long-term fluctuations in hail incidences in the United States. *J. Climate*, **13**, 658–664, doi:10.1175/1520-0442(2000)013<0658:LTFIHI>2.0.CO;2.

China Meteorological Administration, 2012: Chinese meteorological disasters. *Yearbook 2012*, Meteorological Press, 10–30.

Cintineo, J. L., T. M. Smith, V. Lakshmanan, H. E. Brooks, and K. L. Ortega, 2012: An objective high-resolution hail climatology of the contiguous United States. *Wea. Forecasting*, **27**, 1235–1248, doi:10.1175/WAF-D-11-00151.1.

Ding, Y., Z. Wang, and Y. Sun, 2008: Inter-decadal variation of the summer precipitation in east China and its association with decreasing Asian summer monsoon. Part I: Observed evidences. *Int. J. Climatol.*, **28**, 1139–1161, doi:10.1002/joc.1615.

Doswell, C. A., III, H. E. Brooks, and R. A. Maddox, 1996: Flash flood forecasting: An ingredients-based methodology. *Wea. Forecasting*, **11**, 560–581, doi:10.1175/1520-0434(1996)011<0560:FFFAIB>2.0.CO;2.

Fu, Y., G. Liu, G. Wu, R. Yu, Y. Xu, Y. Wang, R. Li, and Q. Liu, 2006: Tower mast of precipitation over the central Tibetan Plateau summer. *Geophys. Res. Lett.*, **33**, L05802, doi:10.1029/2005GL024713.

Huth, R., 1993: An example of using obliquely rotated principal components to detect circulation types over Europe. *Meteor. Z.*, **2**, 285–293.

——, 1996a: An intercomparison of computer-assisted circulation classification methods. *Int. J. Climatol.*, **16**, 893–922, doi:10.1002/(SICI)1097-0088(199608)16:8<893::AID-JOC51>3.0.CO;2-Q.

——, 1996b: Properties of the circulation classification scheme based on the rotated principal component analysis. *Meteor. Atmos. Phys.*, **59**, 217–233, doi:10.1007/BF01030145.

——, 2000: A circulation classification scheme applicable in GCM studies. *Theor. Appl. Climatol.*, **67**, 1–18, doi:10.1007/s007040070012.

——, C. Beck, A. Philipp, M. Demuzere, Z. Ustrnul, M. Cahynová, and O. E. Tveito, 2008: Classifications of atmospheric circulation patterns. *Ann. N. Y. Acad. Sci.*, **1146**, 105–152, doi:10.1196/annals.1446.019.

Ji, X., S. Ma, and Y. Ding, 2007: Analysis of disastrous hail weather in Ningxia in recent 40 years (in Chinese). *Ziran Zaihai Xuebao*, **16**, 24–28.

Jiang, J., and X. Xiang, 1996: Spatial and temporal distributions of severe mesoscale convective systems on Tibetan Plateau in summer (in Chinese). *J. Appl. Meteor. Sci.*, **7**, 474–478.

Johnson, A. W., and K. E. Sugden, 2014: Evaluation of sounding-derived thermodynamic and wind-related parameters associated with large hail events. *Electron. J. Severe Storms Meteor.*, **9** (5), 1–42.

Kapsch, M.-L., M. Kunz, R. Vitolo, and T. Economou, 2012: Long-term trends of hail-related weather types in an ensemble of regional climate models using a Bayesian approach. *J. Geophys. Res.*, **117**, D15107, doi:10.1029/2011JD017185.

Khain, A., A. Pokrovsky, M. Pinsky, A. Seifert, and V. Phillips, 2004: Simulation of effects of atmospheric aerosols on deep turbulent convective clouds using a spectral microphysics mixed-phase cumulus cloud model. Part I: Model description and possible applications. *J. Atmos. Sci.*, **61**, 2963–2982, doi:10.1175/JAS-3350.1.

——, D. Rosenfeld, and A. Pokrovsky, 2005: Aerosol impact on the dynamics and microphysics of deep convective clouds. *Quart. J. Roy. Meteor. Soc.*, **131**, 2639–2663, doi:10.1256/qj.04.62.

Kim, C., and X. Ni, 2014: Climatology of hail in North Korea (in Chinese). *Acta Sci. Nat. Univ. Pekin.*, **51**, 437–443.

Klotzbach, P. J., R. A. Pielke Sr., R. A. Pielke Jr., J. R. Christy, and R. T. McNider, 2009: An alternative explanation for differential temperature trends at the surface and in the lower troposphere. *J. Geophys. Res.*, **114**, D21102, doi:10.1029/2009JD011841.

Kunz, M., J. Sander, and C. Kottmeier, 2009: Recent trends of thunderstorm and hailstorm frequency and their relation to atmospheric characteristics in southwest Germany. *Int. J. Climatol.*, **29**, 2283–2297, doi:10.1002/joc.1865.

Liu, Q. G., and M. C. Tang, 1966: Climatological characteristics of hail in China (in Chinese). *Acta Geogr. Sin.*, **32**, 48–65.

Liu, X., and B. Chen, 2000: Climatic warming in the Tibetan Plateau during recent decades. *Int. J. Climatol.*, **20**, 1729–1742, doi:10.1002/1097-0088(20001130)20:14<1729::AID-JOC556>3.0.CO;2-Y.

Loftus, A. M., and W. R. Cotton, 2014: Examination of CCN impacts on hail in a simulated supercell storm with triple-moment hail bulk microphysics. *Atmos. Res.*, **147–148**, 183–204, doi:10.1016/j.atmosres.2014.04.017.

Myoung, B., and J. W. Nielsen-Gammon, 2010: The convective instability pathway to warm season drought in Texas. Part I: The role of convective inhibition and its modulation by soil moisture. *J. Climate*, **23**, 4461–4473, doi:10.1175/2010JCLI2946.1.

Noppel, H., U. Blahak, A. Seifert, and K. D. Beheng, 2010: Simulations of a hailstorm and the impact of CCN using an advanced two-moment cloud microphysical scheme. *Atmos. Res.*, **96**, 286–301, doi:10.1016/j.atmosres.2009.09.008.

Philipp, A., and Coauthors, 2010: COST733CAT—A database of weather and circulation type classifications. *Phys. Chem. Earth*, **35**, 360–373, doi:10.1016/j.pce.2009.12.010.

——, C. Beck, R. Huth, and J. Jacobeit, 2014: Development and comparison of circulation type classifications using the COST 733 dataset and software. *Int. J. Climatol.*, **36**, 2673–2691, doi:10.1002/joc.3920.

Richman, M. B., 1986: Rotation of principal components. *J. Climatol.*, **6**, 293–335, doi:10.1002/joc.3370060305.

Rosinski, J., and T. C. Kerrigan, 1969: The role of aerosol particles in the formation of raindrops and hailstones in severe thunderstorms. *J. Atmos. Sci.*, **26**, 695–715, doi:10.1175/1520-0469(1969)26<695:TROAPI>2.0.CO;2.

Schuster, S. S., R. J. Blong, and M. S. Speer, 2005: A hail climatology of the greater Sydney area and New South Wales, Australia. *Int. J. Climatol.*, **25**, 1633–1650, doi:10.1002/joc.1199.

Thielen, J., and A. Gadian, 1997: Influence of topography and urban heat island effects on the outbreak of convective storms under unstable meteorological conditions: A numerical study. *Meteor. Appl.*, **4**, 139–149, doi:10.1017/S1350482797000303.

Tippett, M., J. T. Allen, V. A. Gensini, and H. E. Brooks, 2015: Climate and hazardous convective weather. *Curr. Climate Change Rep.*, **1**, 60–73, doi:10.1007/s40641-015-0006-6.

Tuovinen, J. P., A. J. Punkka, J. Rauhala, H. Hohti, and D. M. Schultz, 2009: Climatology of severe hail in Finland: 1930–2006. *Mon. Wea. Rev.*, **137**, 2238–2249, doi:10.1175/2008MWR2707.1.

Vinet, F., 2001: Climatology of hail in France. *Atmos. Res.*, **56**, 309–323, doi:10.1016/S0169-8095(00)00082-X.

Wang, Y., and L. Zhou, 2005: Observed trends in extreme precipitation events in China during 1961–2001 and the associated changes in large-scale circulation. *Geophys. Res. Lett.*, **32**, L09707, doi:10.1029/2005GL023769.

Wang, Z. W., Y. G. Zhang, H. Z. Liu, W. F. Ao, and Z. Huang, 2010: Analyses on weather characters of hail event in Beijing with Mongolia cold vortex (in Chinese). *Plateau Meteor.*, **29**, 763–777.

Xie, B., Q. Zhang, and Y. Wang, 2008: Trends in hail in China during 1960–2005. *Geophys. Res. Lett.*, **35**, L13801, doi:10.1029/2008GL034067.

Yu, M., X. Wang, and J. Guo, 2004a: Characteristic analysis on circulation pattern of systematic hail weather processes and satellite cloud image in Xinjiang (in Chinese). *Plateau Meteor.*, **29**, 787–794.

Yu, R., B. Wang, and T. Zhou, 2004b: Tropospheric cooling and summer monsoon weakening trend over East Asia. *Geophys. Res. Lett.*, **31**, L22212, doi:10.1029/2004GL021270.

Zhang, C., Q. Zhang, and Y. Wang, 2008: Climatology of hail in China: 1961–2005. *J. Appl. Meteor. Climatol.*, **47**, 795–804, doi:10.1175/2007JAMC1603.1.

Zhang, J. P., and Coauthors, 2012: The impact of circulation patterns on regional transport pathways and air quality over Beijing and its surroundings. *Atmos. Chem. Phys.*, **12**, 5031–5053, doi:10.5194/acp-12-5031-2012.

Zhao, C., X. Tie, and Y. Lin, 2006: A possible positive feedback of reduction of precipitation and increase in aerosols over eastern central China. *Geophys. Res. Lett.*, **33**, L11814, doi:10.1029/2006GL025959.